Exploring the edges of visual space: The influence of visual boundaries on peripheral localization

Francesca C. Fortenbaugh
Veterans Administration, Martinez, USA, &
Department of Psychology, University of California, Berkeley, USA

Shradha Sanghvi
School of Optometry, University of California, Berkeley, USA

Michael A. Silver
School of Optometry, University of California, Berkeley, USA, &
Helen Wills Neuroscience Institute, University of California, Berkeley, USA

Lynn C. Robertson
Veterans Administration, Martinez, USA,
Department of Psychology, University of California, Berkeley, USA, &
Helen Wills Neuroscience Institute, University of California, Berkeley, USA

Previous studies of localization of stationary targets in the peripheral visual field have found either underestimations (foveal biases) or overestimations (peripheral biases) of target eccentricity. In the present study, we help resolve this inconsistency by demonstrating the influence of visual boundaries on the type of localization bias. Using a Goldmann perimeter (an illuminated half-dome), we presented targets at different eccentricities across the visual field and asked participants to judge the target locations. In Experiments 1 and 2, participants reported target locations relative to their perceived visual field extent using either a manual or verbal response, with both response types producing a peripheral bias. This peripheral localization bias was a non-linear scaling of perceived location when the visual field was not bounded by external borders induced by facial features (i.e., the nose and brow), but location scaling was linear when visual boundaries were present. Experiment 3 added an external border (an aperture edge placed in the Goldmann perimeter) that resulted in a foveal bias and linear scaling. Our results show that boundaries that define a spatial region within the visual field determine both the direction of bias in localization errors for stationary objects and the scaling function of perceived location across visual space.

Keywords: visual space, visual boundaries, peripheral localization

Citation: Fortenbaugh, F. C., Sanghvi, S., Silver, M. A., & Robertson, L. C. (2012). Exploring the edges of visual space: The influence of visual boundaries on peripheral localization. *Journal of Vision, 12*(2):19, 1–18, http://www.journalofvision.org/content/12/2/19, doi:10.1167/12.2.19.

Introduction

Without the ability to localize objects in the environment, it would be nearly impossible to perform important functions in everyday life, including obstacle avoidance, wayfinding, or the development of spatial representations to guide behavior. While a significant amount of work has been conducted on localization in depth perception (Cutting & Vishton, 1995; Fortenbaugh, Hicks, Hao, & Turano, 2007; Gibson, 1950; He, Wu, Ooi, Yarbrough, & Wu, 2004; Luneburg, 1950; Ooi, Wu, & He, 2001, 2006; Philbeck, Loomis, & Beall, 1997; Sinai, Ooi, & He, 1998) and localization of moving targets (Hubbard, 2005; Kerzel & Gegenfurtner, 2004; Thornton, 2002), far less is known about the factors that influence how individuals localize stationary objects across the visual field. Visual perception begins with 2D representations of space, and the 3D world in which we live arises only after a significant amount of processing (Palmer, 1999). It is therefore of great importance to understand the principles that guide location perception as a function of eccentricity. Moreover, visual field deficits, such as those occurring from retinal degeneration and cortical damage following brain trauma, affect entire regions of the visual field, not just locations at specific depths. A better understanding of intrinsic biases in the perception of locations across the visual field and the factors that influence these biases in normal vision will therefore elucidate how visual perception changes when parts, but not all, of the visual field are

doi: 10.1167/12.2.19 Received August 16, 2011; published February 20, 2012 ISSN 1534-7362

lost (e.g., Temme, Maino, & Noell, 1985; Turano, 1991; Wittich, Faubert, Watanabe, Kapusta, & Overbury, 2011).

Foveal and peripheral biases in peripheral localization

One of the initial studies in this area (Mateeff & Gourevich, 1983) found that participants display a foveal bias when estimating locations of peripheral stationary targets, with perceived locations being increasingly displaced toward the fovea as the true target eccentricity increases. Since then, numerous studies have replicated the finding of a foveal bias (Adam, Davelaar, van der Gouw, & Willems, 2008; Fortenbaugh & Robertson, 2011; Hubbard & Ruppel, 2000; Kerzel, 2002; Müsseler & Van der Heijden, 2004; Müsseler, van der Heijden, Mahmud, Deubel, & Ertsey, 1999; Rose & Halpern, 1992; van der Heijden, van der Geest, de Leeuw, Krikke, & Müsseler, 1999). Notably, the studies reporting a foveal localization bias used either closed-loop pointing responses, such as moving a mouse cursor to the perceived target location (Adam et al., 2008; Hubbard & Ruppel, 2000), or perceptual responses, as classified by Uddin (2006): verbal report of perceived target location (Fortenbaugh & Robertson, 2011) or key presses indicating the perceived relative positions of targets (Kerzel, 2002). However, other studies (Bock, 1993; Bruno & Morrone, 2007; Enright, 1995) employing open-loop pointing movements toward perceived locations of stationary targets (where visual feedback regarding the position of the arm is not available) have found evidence for a peripheral bias, with targets being mislocalized away from the fovea.

One explanation that has been proposed to account for the discrepancy between studies reporting a foveal bias and those reporting a peripheral bias is the manner in which participants respond (Bruno & Morrone, 2007; Uddin, 2006). In particular, it has been suggested that open-loop motor responses (e.g., pointing without visual feedback) are more likely to show a peripheral bias, while both closed-loop motor responses (such as moving a mouse cursor on a computer monitor) and perceptual responses (such as verbal reports) are more likely to result in foveal biases. This account suggests that peripheral biases may result from errors in the motor system or in the transformation of spatial information from a retinotopic reference frame to an egocentric arm- or hand-based motor reference frame.

Of special interest to the current study are the results of Temme et al. (1985), in which a peripheral bias was found, but the response mode does not fit well within the open-loop motor explanation. In this study, a Goldmann perimeter[1] was used to present a target light at 10° intervals between the central visual field and the edge of the visual field, along the cardinal and oblique meridians. Participants reported perceived target location by drawing a hash mark along a line printed on a sheet of paper, where the center of the line corresponded to the point of fixation and the edges corresponded to the perceived visual field edges along the meridian that was being tested. In this study, participants overestimated target eccentricity at all locations, and errors were largest in the near periphery and decreased for target locations closer to the edges of the visual field.

Although the response mode used in Temme et al.'s (1985) study was motor based, it was not an open-loop pointing task. Participants first needed to assess the perceived location of the target on a scale bounded by the point of fixation on one end and the perceived edge of their visual field on the other. This scale was then transformed to match the line on the response sheets. The fact that peripheral biases were found in this study suggests that such biases cannot be attributed solely to errors in the motor system.

Resolving discrepancies: The influence of visual boundaries. The present study investigates an alternative explanation for foveal and peripheral biases in the localization of stationary targets in the visual periphery. In previous studies reporting a peripheral bias, strong external visual borders (such as the edges of a computer monitor) were not present (Bock, 1993; Enright, 1995; Temme et al., 1985). In contrast, the majority of studies that found a foveal bias either presented the stimuli within a space defined by the edges of a computer monitor (Adam et al., 2008; Bocianski, Müsseler, & Erlhagen, 2008; Fortenbaugh & Robertson, 2011; Kerzel, 2002; Tsal & Bareket, 2005; Uddin, Kawabe, & Nakamizo, 2005a) or obtained distance judgments relative to a visible reference line (Mateeff & Gourevich, 1983). It has previously been suggested that when target locations can be encoded in either an extrinsic or intrinsic reference frame, extrinsic reference frames defined by external visual cues take precedence (Lemay & Stelmach, 2005; Sheth & Shimojo, 2004). In order to explain peripheral and foveal biases, it is therefore important to consider not only the type of reference frame used but also the metrics (i.e., distance functions) within these reference frames that define coordinate systems for localizing stimuli.

Thus, another way to interpret the results of Temme et al. (1985) is that the borders of the visual field provide a natural boundary with which to define a metric of visual space within an egocentric reference frame. This would be similar to the use of external visual boundaries to define relative positions in extrinsic (allocentric) reference frames. However, for the same target locations, there may be different metrics associated with intrinsic versus external visual field boundaries. In three experiments, we tested the hypothesis that scaling location judgments relative to one's perceived visual field extent leads to an expansion in perceived eccentricity for stationary targets in perifoveal and peripheral visual field locations, while

the introduction of external visual boundaries modifies the scaling and causes a switch from peripheral to foveal bias. Moreover, we show that the type of border used to make judgments modulates the scaling of space across eccentricity across multiple response types.

An additional motivation for Experiment 1 was to determine whether Temme et al.'s (1985) results would be replicated using the same design, given that no other studies in the peripheral localization literature have used a similar paper-and-pencil method. We also sought to extend the findings of Temme et al. by quantifying the scaling of locations along each axis in order to test for systematic differences in the metric across axes, depending on the natural visual boundaries of the face.

Experiment 1

Methods

Participants

Six participants (four females, mean age: 21.7 ± 2.6 years) participated in this experiment. All participants had 20/20 visual acuity, either without any optical correction or with optical correction by contact lenses. Participants were excluded if they wore eyeglasses, as these can artificially restrict the visual field along the horizontal axis (Steel, Mackie, & Walsh, 1996). Eye disease of any kind was also an exclusion criterion. This research was approved by the Committee for the Protection of Human Subjects at the University of California, Berkeley, and followed the tenets of the Declaration of Helsinki.

Materials and procedure

Following the procedure of Temme et al. (1985), a Haag-Streit Goldmann projection perimeter (Figure 1) was used to obtain an initial measurement of the full monocular visual field extent for each participant using standard clinical procedures. This was performed using the standard III4e test target (0.44° test spot at a viewing distance of 30 cm; 318 cd/m^2 on a background luminance of 10 cd/m^2). As in Temme et al., only the right eye was tested, while the left eye was occluded. Participants maintained fixation on a dot located in the opening of the telescope at the center of the half-dome while the experimenter projected the target light in the far periphery and then slowly moved it toward the fovea. Participants pressed a button that elicited a tone as soon as they detected the light in the periphery. Upon hearing the tone, the experimenter, situated on the other side of the perimeter, marked the location of the target dot on a chart. After determining the participant's visual field extent, the experimenter briefly flashed the target at the boundary location along each of the four axes to remind participants of the locations of the edges of their visual field. Given that naive observers participated in the experiments in this paper, this procedure assured that all participants were familiar with the concept of visual field extent and were aware of the boundaries of their monocular visual field.

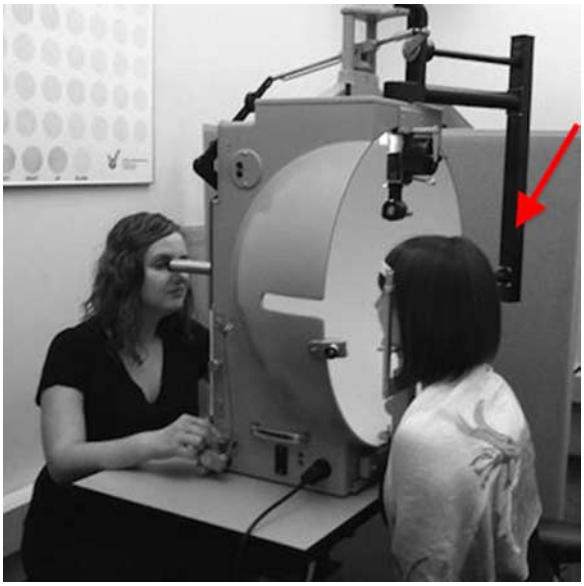

Figure 1. Photograph of the Goldmann perimeter. The participant is seated on the right, facing the dome, and the experimenter is seated on the left. The experimenter controls the position of the target light by moving the projector (indicated by red arrow) via a bar with their left hand. This bar has a marker on the experimenter's side that indicates the target light's location on a chart in polar coordinates. The target light is presented by pressing a lever with the right hand. Fixation is monitored through a telescope.

The Goldmann perimeter was then used to present targets at various locations. The III4e target was presented at 10° intervals, from 10° eccentricity to the edge of the participant's visual field, along the four cardinal axes. Different pre-generated random sequences were used for each participant to control target presentation along the chosen meridian, with each location being tested five times. As target presentation times are not automated in Goldmann perimeters, the experimenter manually controlled target locations and presentation times (see Figure 1). The same experimenter conducted all testing. Prior to testing participants, 200 measurements of presentation time were recorded, and the average presentation time was 176.8 ms (*SD* = 25.5 ms). Throughout testing, participants maintained fixation at the center of the perimeter, where a small telescope was located that allowed the experimenter, seated on the other side of the dome, to view the participant's eye and to ensure that fixation was maintained. Prior to each trial, the experimenter adjusted the projector arm to the correct position to present the target for that trial. Then, the experimenter verbally indicated to

the participant that the next trial was about to begin, and once the participant established fixation, the target was then briefly presented. Eye position was continually monitored throughout target presentation by the experimenter, and any trial in which fixation was not maintained was repeated.

Participants indicated their response on a sheet of paper (20.3 × 7.6 cm) that was placed on a table on the side corresponding to the participant's preferred hand. A black line 180 mm in length was centered on this paper, with a 5-mm hash mark bisecting the line. Following target presentation, participants indicated perceived target location by drawing a line on the response sheet. They were told that the central hash mark on the response sheet corresponded to the fixation point in the perimeter and that the ends of the line corresponded to the perceived edges of their visual field along the meridian being tested. When generating their response, participants were instructed to sit back from the perimeter chin rest and to turn toward the side table to mark the response sheet. After each response, participants were realigned in the perimeter before continuing to the next trial.

Testing was conducted in two 1-h sessions on different days, with either the horizontal or vertical meridian being tested on a given day. Testing of the horizontal and vertical meridians was separated in order to follow the methodology of Temme et al. (1985) as well as for testing convenience. In each session, the orientation of the response sheets was adjusted to align with the meridian being tested. For horizontal meridian testing, sheets were oriented such that the response line was also horizontally oriented, and the response line was vertically oriented when the vertical meridian was tested. Testing order was counterbalanced across participants.

Results

Localization errors

The mean measured monocular visual extents of the participants' right eyes were: temporal axis = 89° ± 3°, nasal axis = 57° ± 3°, inferior axis = 70° ± 3°, and superior axis = 48° ± 6°. We performed the same data analyses as Temme et al. (1985). First, the distance of the response line from the central hash mark was measured in millimeters. This value was converted to percentage of the line length, representing the estimated percentage of visual field extent. True target position was expressed as percentage of visual field extent by dividing the target eccentricity by the measured visual field extent for the axis being tested, as visual field extents varied across participants. Figure 2 shows the average errors in units of percentage of visual field extent as a function of target eccentricity in degrees for the vertical and horizontal meridians. Errors were defined as the estimated percentage of visual field extent minus the true percentage of visual field extent. Thus, positive values indicate overestimation, or peripheral bias, while negative values indicate underestimation, or foveal bias.

A 4 (Axis, upper and lower vertical meridians, nasal and temporal horizontal meridians) × 5 (Eccentricity) repeated measures ANOVA was used to analyze the error scores for the five most central eccentricities for each of the four axes. These eccentricities were chosen because they were represented on all axes. There was no main effect of Axis ($F(3,6) = 1.25$, $p = 0.37$) or Axis × Eccentricity interaction ($F(12,24) = 0.65$, $p = 0.78$). However, the main effect of Eccentricity was significant ($F(4,8) = 6.66$, $p = 0.012$). Trend analysis of the Eccentricity factor indicated a significant quadratic trend

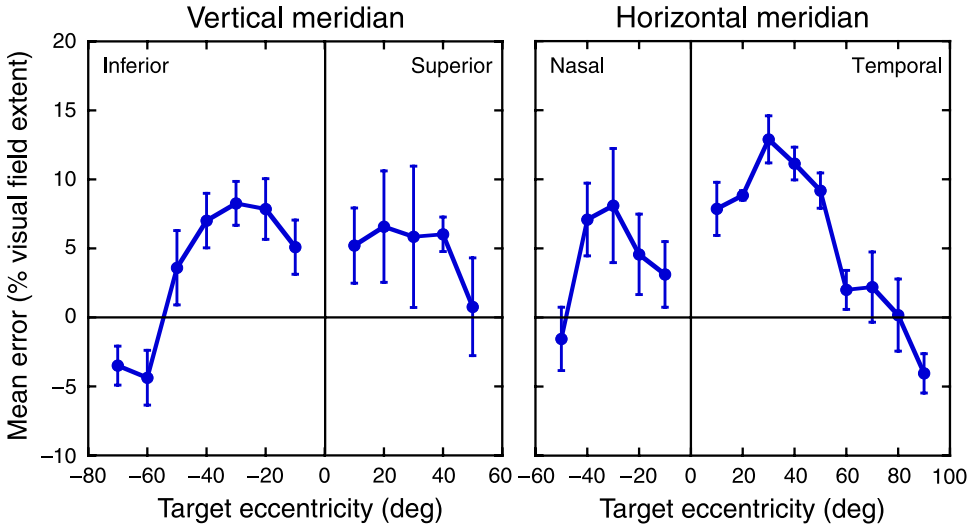

Figure 2. Experiment 1: Localization errors. Mean errors in percent of visual field extent for the vertical and horizontal meridians as a function of target eccentricity. Error bars represent *SEM*. Solid horizontal lines at zero represent expected performance if no distortion exists.

($F(1,2) = 33.77$, $p = 0.028$), and the linear and cubic trends were not significant ($p > 0.23$ for both). Figure 2 shows that the quadratic trend is characterized by an inverted U-shaped function, with errors showing maximal peripheral bias at approximately 20°–30° eccentricity.

Spatial uncertainty in perceived location

As visual acuity and contrast sensitivity are known to decrease substantially in the periphery (Low, 1951; Randall, Brown, & Sloan, 1966; To, Regan, Wood, & Mollon, 2011), it is possible that target localization errors may reflect increased spatial uncertainty in the far periphery. We estimated spatial uncertainty by calculating standard deviations of the five repeats at each target location. Figure 3 shows the mean standard deviations of the errors as a function of target eccentricity along the four axes tested. As with the magnitude errors, a 4 (Axis) × 5 (Eccentricity) repeated measures ANOVA was conducted on the standard deviations of the errors for the five most foveal eccentricities tested. No significant main effects or interaction terms were found ($F < 1$ for all).

Magnitude scaling

As visual field extents vary across axes and across individuals, we normalized both target eccentricity and participants' responses to assess the scaling of localization responses independent of the absolute size of the visual field. Following Temme et al. (1985), the farthest point tested along each axis for each participant was considered to be 100% target eccentricity, and all other visual field locations were normalized relative to this eccentricity. We also normalized responses by computing the average response to the most peripheral target tested for each axis and each participant and defining this average response as 100% maximum. Average responses to all other target eccentricities were then scaled relative to this maximum response for each participant and axis. This normalization of both the maximum eccentricity tested and the maximum response was used to examine the linearity of scaling of responses.

Figure 4 shows the means of the percentage of maximum response as a function of the percentage of maximum eccentricity for the vertical and horizontal meridians, respectively, for each participant. If participants accurately scaled target locations relative to a fixed maximal visual field size, then all the points would fall on the black line that indicates a linear relationship between perceived and actual target eccentricity. As is evident in Figure 4, the data points from the six observers are primarily above the line, indicating an overestimation of perceived eccentricity beyond that due to a factor that is constant across the visual field, consistent with a non-linear peripheral bias for targets presented in the peripheral visual field.

While the normalization procedure shown in Figure 4 provides evidence of non-linear scaling that is consistent with the type of errors reported by Temme et al. (1985; see Figure 8), this approach cannot quantify the underlying metric. To do this, we used a hierarchical modeling scheme to fit a two-parameter power function relating the non-normalized magnitude estimate to the target eccentricity for each trial (with target eccentricity expressed in units of percent of participant's visual field extent along the axis tested). A predefined origin (the fixation dot located inside the telescope at the center of the dome) was present on every trial, eliminating the need for a constant parameter in the model. For every participant, two power functions (Equation 1) were fit to the raw magnitude

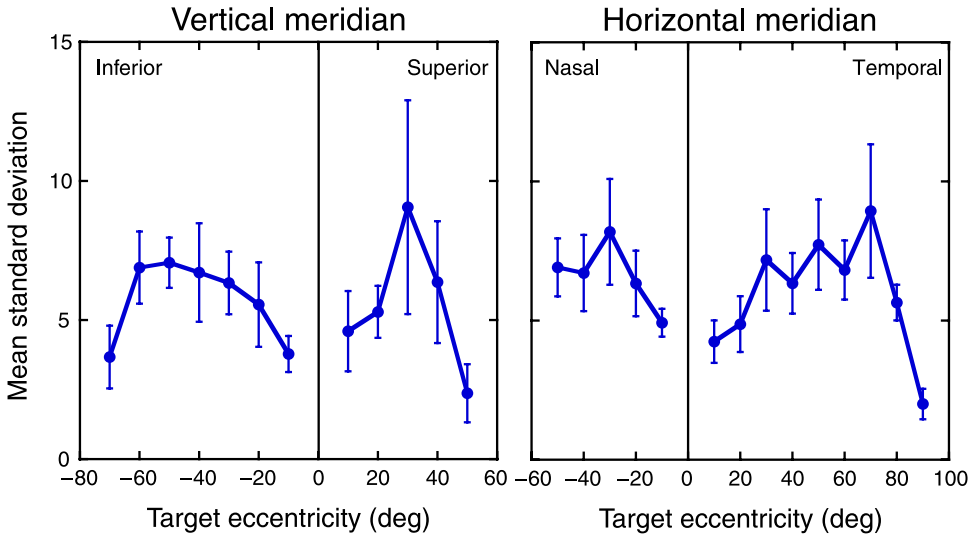

Figure 3. Experiment 1: Spatial uncertainty. Mean standard deviations of the errors in units of percent of visual field extent for vertical and horizontal meridians as a function of target eccentricity. Error bars represent *SEM*.

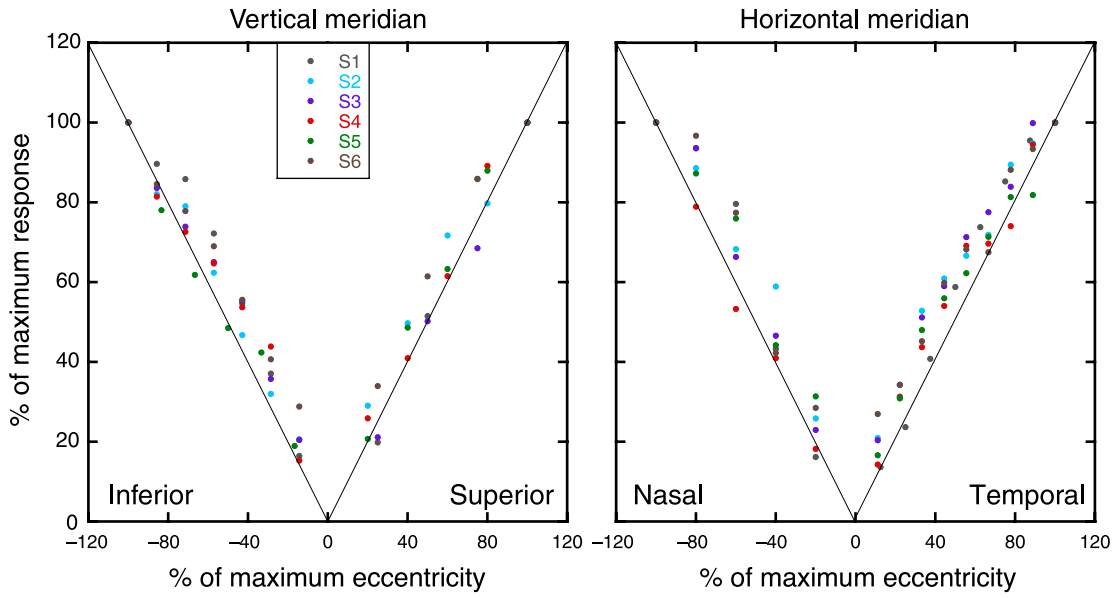

Figure 4. Experiment 1: Normalized magnitude estimates; *y*-axis: mean magnitude estimates for each participant, normalized by the mean maximum magnitude estimate reported by that participant for each of the four cardinal axes; *x*-axis: percent of the maximum target eccentricity tested along each axis. Solid lines show expected performance if scaling of responses along each axis was linear and unbiased.

estimates for all eccentricities tested, separately for each of the four axes:

$$J = \lambda D^{\alpha}. \quad (1)$$

In this equation, J is the estimated target magnitude, D is the actual target magnitude, λ is the slope parameter that represents a global scaling factor that compresses or expands all values by a constant amount proportional to the actual target magnitude, and α is the exponent parameter that quantifies the linearity of the function. An α value of 1 indicates a linear relationship between magnitude estimate and target location, while deviation from a value of 1 indicates that estimates do not scale linearly across eccentricity. For every participant and axis tested (6 participants and 4 axes = 24 combinations), two models were fit, one in which both the λ and α parameters were free to vary and one in which the α parameter was fixed at a value of 1 (GraphPad Prism, San Diego, CA). The increase in the amount of variance explained by the two-parameter model compared to the null one-parameter model was quantified with an F ratio, taking into account differences in degrees of freedom in the two models (Motulsky & Christopoulos, 2004). The two-parameter model was determined to provide a significantly better fit than the null one-parameter model for a given participant/axis combination when the F ratio had a corresponding $p \leq 0.05$. For the one-parameter model, the average percent variance accounted for was 88% (range: 80 to 95 across participant/axis combinations), while the two-parameter model accounted for an average percent variance of 92% (range: 82 to 96 across participant/axis combinations). Across the four axes for each of the six participants, the two-parameter model provided a significantly better fit than the one-parameter model for 15 out of 24 (63%) participant/axis combinations. Moreover, 5 out of 6 (83%) participants showed significantly better fits for the two-parameter model along the temporal and inferior axes. Given these findings, estimates from the two-parameter model were used in further analyses.

Figure 5 shows the mean slope and exponent parameters for each of the four cardinal axes. If estimated and actual target eccentricities were identical, both of these parameters would have a value of 1. Two one-way repeated measures ANOVAs were conducted on the parameter estimates. There was a trend in the main effect of Axis for the slope parameter ($F(3,15) = 3.10$, $p = 0.06$) and a significant main effect of Axis for the exponent parameter ($F(3,15) = 3.24$, $p = 0.05$). One-sample t tests were used to determine whether the slope and exponent parameters for the four axes differed significantly from a hypothetical mean of 1 (Sidak–Bonferonni correction for multiple comparisons, $\alpha_{S-B} = 0.013$). For both the slope and exponent estimates, only the inferior and temporal axes were significantly different than 1, with mean slopes greater than 1 and mean exponents less than 1 (mean slope: temporal = 3.29, $p = 0.003$; inferior = 2.69, $p = 0.008$; nasal = 2.16, $p = 0.043$; superior = 1.81, $p = 0.129$; mean exponent: temporal = 0.75, $p = 0.001$; inferior = 0.78, $p = 0.001$; nasal = 0.86, $p = 0.034$; superior = 0.90, $p = 0.144$). These results demonstrate that the degree of peripheral bias was least prominent along the superior and

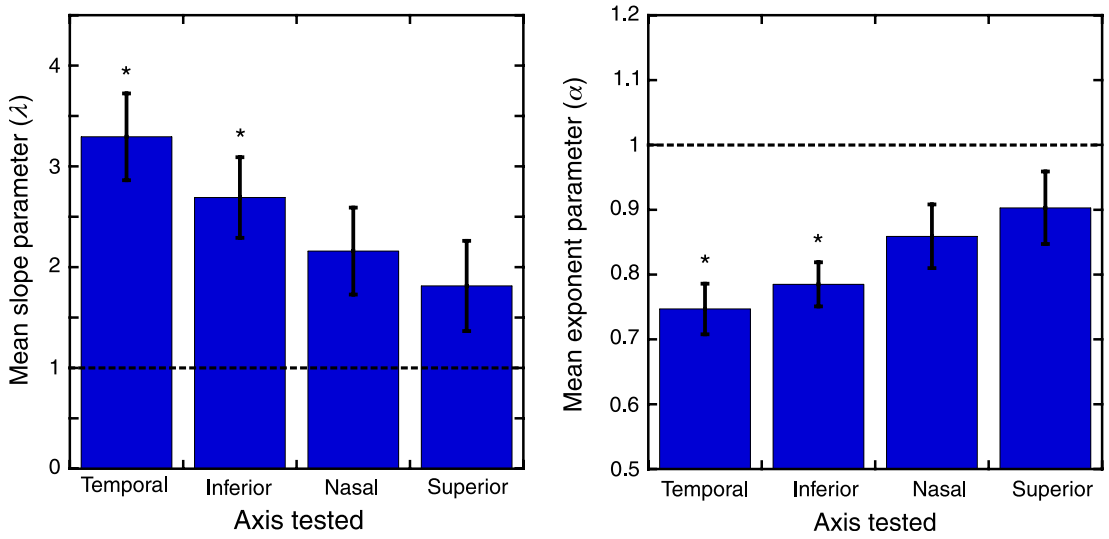

Figure 5. Experiment 1: Power function parameters. Mean estimated slope and exponent parameters as a function of axis tested, obtained from fitting individual participant magnitude estimates with the two-parameter function $J = \lambda D^{\alpha}$. Error bars represent *SEM*. Dotted lines at one represent expected performance if perceived and actual eccentricities were identical across tested locations. Asterisks indicate that the mean value is significantly different from 1, following correction for multiple comparisons.

nasal axes and largest along the temporal and inferior axes, both of which show significant deviations from a linear scaling.

Discussion

Replicating Temme et al. (1985), we found an overall peripheral bias for both directions of horizontal as well as vertical dimensions. However, the magnitude of the errors was not constant across eccentricity. Trend analyses showed a significant inverted U-shaped function, with errors peaking at 20°–30° eccentricity. Moreover, there were differences in scaling across the four axes, as evident by the main effect of axis for the exponent parameters and differences in linearity across the axes, as demonstrated by the one-sample *t* tests. Results from these analyses show that the degree of peripheral bias was most prominent along the temporal axis, followed by the inferior axis, then nasal and superior axes.

These findings extend those of Temme et al. (1985) in that they more fully characterize the type of scaling used in estimating target location. This was accomplished by fitting power functions to the mean estimated eccentricities for each participant along the four cardinal axes. Unlike the linear regression analyses employed by Temme et al., the power functions used to fit the data here had two free parameters: a slope parameter, reflecting a global scaling factor, and an exponent parameter, quantifying the linearity of the scaling. Power functions with an exponent value that was not fixed at 1 accounted for the scaling across eccentricity better than linear fits, indicating that, in general, participants did not use a linear metric in scaling responses across the visual field.

Importantly, the results further show that the type of scaling varied across the axis tested. Neither the slope nor the exponent parameters were significantly different from 1 along the superior and nasal axes, suggesting that the degree of peripheral bias is relatively stable across eccentricity for these two axes and indicating a linear scaling metric for these axes. For the inferior and temporal axes, a non-linear metric was observed, with slope parameters significantly greater than 1 and exponent parameters significantly less than 1.

The slope and exponent parameters showed opposing patterns across the four axes (Figure 5). These parameters capture the degree to which the magnitude of peripheral biases varied across eccentricity for the four axes. In particular, the largest slopes are found for the temporal axis, which also exhibited the greatest overestimations in perceived location. However, as seen in Figure 2, peripheral biases peaked in the mid-periphery and were absent in the far periphery. This non-linearity in peripheral bias as a function of eccentricity results in the exponent parameter having a value less than 1. In contrast, the magnitude of the peripheral bias was relatively smaller and more consistent across eccentricity for the superior axis, resulting in a smaller slope parameter and a larger exponent parameter, both of which were not significantly different than a value of 1. Collectively, then, the results support the existence of two distinct scaling functions across the four axes.[2]

Reduced eccentricity overestimation in the superior and nasal visual fields may be due to visual field borders arising from facial anatomical constraints. In particular, the superior and nasal fields are bounded by the upper brow and nose (external borders), while the temporal and inferior fields are typically not constrained by facial features. Thus, the visual field boundaries along these

axes are intrinsic. One possibility is that the presence of these facial boundaries reduces uncertainty in the location of the edge of the visual field, leading to reduced peripheral bias and a linear scaling metric. However, analysis of the standard deviations argues against this interpretation. As seen in Figure 3, standard deviations were comparable in size across the four axes. For all axes but the nasal axis, the smallest standard deviations are associated with the most peripheral targets, demonstrating that participants showed the least spatial uncertainty for target locations near their visual field extents. Moreover, the nasal axis contains the strongest external visual border (the nose), yet standard deviations remain high for this axis for the most peripheral eccentricities tested. Finally, if the absence of external visual field boundaries led to greater uncertainty in target positions along the inferior and temporal axes, standard deviations should have been larger for more eccentric locations along these axes, but this was not the case.

An additional argument against an uncertainty-based explanation of our results is based on the magnitude of the localization errors. Had participants been more uncertain of target locations along the inferior and temporal axes, there should have been greater variability in responses in both directions (overestimations and underestimations), resulting in a reduction in the mean bias for these axes. In contrast, larger peripheral biases were observed along these axes than the superior and nasal axes. These results therefore suggest that differences in spatial uncertainty across the four axes tested cannot explain the differences in scaling.

Results from the normalization procedure (Figure 4) also argue against systematic differences in mislocalization of visual field extent driving the peripheral bias that we observed across all axes. Here, for each participant and each axis, all responses were scaled relative to the maximum response, and target eccentricities were scaled relative to the maximum eccentricity tested. If participants underestimated the extent of their visual field along the inferior and temporal axes due to decreased visibility of intrinsic visual field boundaries, our normalization procedure would correct for this. As is evident in Figure 4, even if participants had underestimated their visual field extent, scaling was still non-linear and/or showed additional peripheral bias in estimated locations across the range of eccentricities tested (i.e., estimated magnitudes were predominantly above the line that represents a linear scaling of perceived eccentricity relative to the maximum eccentricity tested). This rules out an explanation of peripheral localization bias based on inward shifts of the perceived visual field boundary.

Our findings support an interpretation in which peripheral biases and non-linear scaling metrics are evident when localization occurs in spaces without clearly visible boundaries (i.e., when scaling is made relative to intrinsic visual field boundaries). In these cases, participants must localize targets within a retinotopic, egocentric reference frame. Indeed, the absence of clear external boundaries distinguishes previous studies on peripheral localization that reported peripheral biases (Bock, 1993; Enright, 1995; Temme et al., 1985) from those that have found foveal biases (Hubbard & Ruppel, 2000; Kerzel, 2002; Mateeff & Gourevich, 1983). The presence or absence of external visual boundaries also accounts for the different localization biases found across the four axes tested in the present study. However, the unique paper-and-pencil response type used in the present study and Temme et al. (1985) may also have influenced participants' magnitude estimates. We therefore conducted Experiment 2, in which verbal responses were used to indicate perceived target location. We also added a binocular condition that eliminated the border of the nose that was present in the monocular target presentation in Experiment 1. We hypothesized that in the monocular (right eye) condition, response scaling along the nasal (left) axis should be linear (as we found in Experiment 1), but that in the binocular condition, removal of the external visual boundary of the nose should result in non-linear scaling along the left axis (as we found for monocular presentation along the temporal (right) axis in Experiment 1).

Experiment 2

Methods

Participants

Twelve healthy undergraduates (9 females; mean age: 21.3 ± 3.9 years) who had not participated in the previous experiment participated in this experiment for course credit. The same exclusion criteria as in Experiment 1 were used.

Materials and procedure

As in Experiment 1, a Goldmann perimeter was used to measure the visual field extent of all participants and to present visual targets, and the same III4e target dot was used for both boundary determination and testing. For the binocular viewing condition, head position was adjusted so that participants could comfortably view the fixation dot in the center of the perimeter. Eye position was monitored via the telescope in the center of the perimeter, which provided a view of the right eye.

For both monocular and binocular conditions, targets were presented at 10° intervals from 10° eccentricity to the edge of the participant's visual field along the four cardinal axes, with trials containing target locations along the horizontal and vertical meridians intermixed within each viewing condition block. All locations were tested five times during a block, and a separate random testing sequence was generated prior to testing for each participant. On each trial, participants generated a verbal

magnitude estimate of the target's location. The estimate ranged between 0 and 100, where 0 corresponded to the point of fixation and 100 corresponded to the edge of the participant's perceived visual field extent. Thus, the magnitude estimates mirrored the manual response in Experiment 1, where the center hash mark corresponded to the point of fixation and the edge of the line corresponded to the edge of the perceived visual field extent. Any trial in which fixation was not maintained was repeated. All participants completed five practice trials before beginning the experiment, and block order (monocular vs. binocular) was counterbalanced across participants.

Results

Localization errors

The mean measured visual extents of the participants' right eyes were: temporal axis = 90° ± 2°, nasal axis = 61° ± 3°, inferior axis = 71° ± 4°, superior axis = 49° ± 8°. The mean visual extents of the binocular visual fields were: right axis = 90° ± 2°, left axis = 89° ± 4°, inferior axis = 71° ± 4°, superior axis = 51° ± 7°. As in Experiment 1, each target eccentricity was converted to percentage of visual field extent, and errors in magnitude estimates were then calculated by subtracting this percentage from the verbal magnitude estimates. Figure 6 shows the mean errors in percent visual field extent as a function of target eccentricity and viewing condition (monocular or binocular) for the vertical and horizontal meridians. For the monocular viewing condition, the results mirror the pattern in Experiment 1: There was a peripheral localization bias, particularly along the temporal (right) and inferior axes. The peripheral bias was much smaller along the nasal (left) axis. In contrast, binocular viewing produced large peripheral biases along the left axis that were similar in magnitude and eccentricity profile to those observed along the right axis. Errors were similar for monocular and binocular viewing along the superior and inferior axes.

A 2 (Viewing Condition) × 4 (Axis) × 5 (Eccentricity) repeated measures ANOVA was conducted on localization errors for the five most central eccentricities, using Greenhouse–Geisser corrections when Mauchly's Test of Sphericity indicated that the assumption of sphericity was not met. As in Experiment 1, these five eccentricities were chosen because they were represented on all axes. There were significant main effects of Eccentricity ($F(1.37,10.93) = 8.23$, $p = 0.01$) and Axis ($F(3,24) = 7.49$, $p = 0.001$). The main effect of Viewing Condition was not significant ($F(1,8) = 0.002$, $p = 0.97$), but the Viewing Condition × Axis interaction was significant ($F(3,24) = 3.06$, $p = 0.05$), as was the Axis × Eccentricity interaction ($F(12,96) = 2.10$, $p = 0.02$). The Viewing Condition × Eccentricity interaction was not significant ($F(4,32) = 0.17$, $p = 0.95$), nor was the three-way interaction ($F(12,96) = 1.25$, $p = 0.26$). Trend analysis of the Eccentricity factor indicated a significant quadratic trend ($F(1,8) = 35.64$, $p < 0.001$), and the linear and cubic trends did not reach significant levels (linear: $p = 0.07$, quadratic: $p = 0.08$). As in Experiment 1, the quadratic trend as a function of eccentricity is characterized by an inverted U-shaped function (Figure 6).

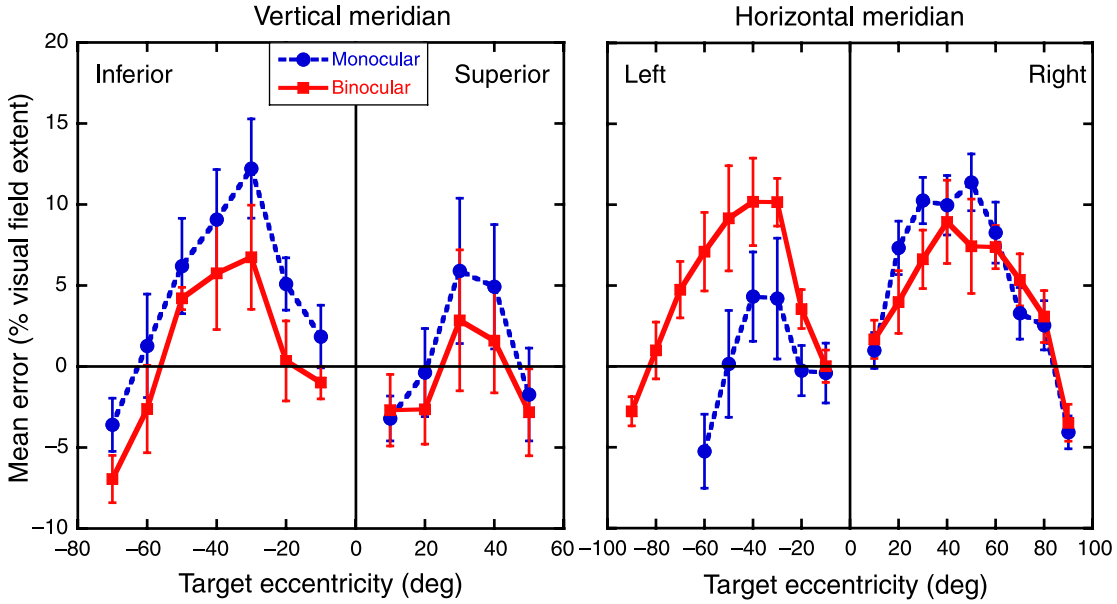

Figure 6. Experiment 2: Localization errors. Mean errors in percent of visual field extent for vertical and horizontal meridians as a function of viewing condition and target eccentricity. Error bars represent *SEM*. Solid horizontal lines at zero represent expected performance if no distortion exists.

Magnitude scaling

The same hierarchical modeling scheme described in Experiment 1 was used to fit the function relating magnitude estimates to actual target locations, expressed in terms of percent of visual field extent. Both one-parameter (exponent fixed at $\alpha = 1$) and two-parameter (exponent was free parameter) functions were tested. The one-parameter model accounted for 90% of average variance (range: 70 to 98), and the two-parameter model accounted for 93% of average variance (range: 82 to 98). Overall, the two-parameter model provided a significantly better fit for 53 of the 96 (55%) combinations of participant (12 subjects), axis (4), and viewing condition (monocular and binocular). Specifically, results showed that the two-parameter model provided a significantly better fit than the null model for all 12 participants in the monocular viewing condition along the temporal axis and a significantly better fit for 10 out of 12 (83%) participants for both the left and right axes in the binocular viewing condition. Thus, estimates from this model were used in subsequent analyses.

Figure 7 shows the mean slope and exponent parameters for each of the four cardinal axes under monocular and binocular viewing conditions. A 2 (Viewing Condition) × 4 (Axis) repeated measures ANOVA indicated that the slopes differed across the four axes ($F(3,33) = 11.46$, $p < 0.001$). While the main effect of Viewing Condition was not significant ($F(1,11) = 0.05$, $p = 0.83$), there was a significant Viewing Condition × Axis interaction ($F(3,33) = 3.16$, $p = 0.04$). One-sample t tests were used to determine whether the slope parameters across the eight conditions differed significantly from a hypothetical mean of 1 using the Sidak–Bonferonni correction for multiple comparisons ($\alpha_{S-B} = 0.006$). For binocular viewing, all axes except the superior axis had mean slopes significantly greater than one (right = 2.27, $p = 0.001$; inferior = 2.28, $p = 0.002$; left = 2.56, $p < 0.001$; superior = 0.99, $p = 0.97$). Like binocular viewing, monocular viewing resulted in mean slopes significantly greater than one for the right and inferior axes but not for the superior axis (right/temporal = 2.91, $p < 0.001$; inferior = 2.50, $p = 0.002$; superior = 1.11, $p = 0.68$). In contrast, the mean slope for the left axis was not significantly different than 1 for monocular viewing (left/nasal = 1.79, $p = 0.050$), demonstrating a difference between monocular and binocular viewing in the scaling of estimates along this axis.

The same pattern was obtained for the estimated exponent parameters. A 2 (Viewing Condition) × 4 (Axis) repeated measures ANOVA, using Greenhouse–Geisser corrections when appropriate, showed a main effect of Axis ($F(3,33) = 23.20$, $p < 0.001$). The main effect of Viewing Condition was not significant ($F(1,11) = 0.36$, $p = 0.56$), but the Viewing Condition × Axis interaction was significant ($F(1.66,18.24) = 3.97$, $p = 0.04$). One-sample t tests were again used to determine whether the exponent parameters across the eight conditions differed significantly from a hypothetical mean of 1 using the Sidak–Bonferonni correction for multiple comparisons ($\alpha_{S-B} = 0.006$). In the binocular viewing condition, all axes except for the superior axis had mean exponent values that were significantly less than 1 (right = 0.84, $p < 0.001$; inferior = 0.84, $p < 0.001$; left = 0.81, $p < 0.001$; superior = 1.15, $p = 0.112$). In the monocular condition, the mean exponent along the left axis was not significantly different than 1 (0.92, $p = 0.082$), further supporting a difference between monocular and binocular viewing in the scaling of estimates along this axis. Mean exponent values for monocular viewing of the other axes were similar to

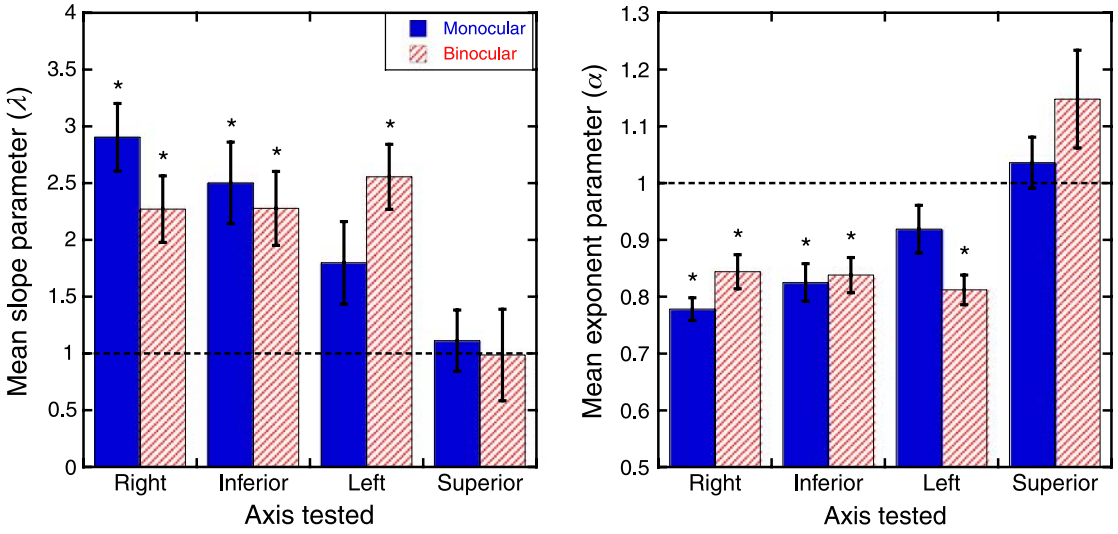

Figure 7. Experiment 2: Power function parameters. Mean estimated slope and exponent parameters as a function of viewing condition and axis tested, obtained from fitting individual magnitude estimates with the two-parameter function $J = \lambda D^{\alpha}$. Error bars represent *SEM*. Dotted lines represent expected performance if the mapping is undistorted and Euclidean. Asterisks indicate that the mean value is significantly different from 1, following correction for multiple comparisons.

those obtained from binocular viewing (right/temporal = 0.78, $p < 0.001$; inferior = 0.82, $p < 0.001$; superior = 1.04, $p = 0.438$).

Discussion

The results of Experiment 2 replicate the peripheral localization bias found in Experiment 1 and, together with the results of Experiment 1, show that for monocular viewing, verbal and motor responses produce the same qualitative pattern of results. Our finding of peripheral bias using verbal magnitude responses is inconsistent with the theory that peripheral biases are found primarily with open-loop motor responses, while closed-loop motor responses and perceptual responses are associated with foveal biases (Uddin, 2006). Rather, our results demonstrate that peripheral biases can also be observed using perceptual tasks such as verbal report and are therefore likely to reflect perceptual distortions. However, some aspects of our data are consistent with an additional peripheral bias introduced by motor, relative to verbal, responses. Peripheral biases tended to be smaller overall in Experiment 2 compared to Experiment 1. In addition, peripheral biases were found in Experiment 1 for both the 10° and 20° target locations across all four axes, particularly along the temporal (right) axis, while in Experiment 2, there was little, if any, bias in estimating targets at these locations (compare Figures 2 and 6). This difference suggests that peripheral biases may be more difficult to detect in computer-based localization tasks, which predominantly test locations less than 20° eccentricity. The larger peripheral biases observed in Experiment 1 compared to Experiment 2 at these eccentricities are also consistent with previous reports that the use of a verbal response eliminated the peripheral bias that was observed with pointing responses for targets located in the central 30° (Bruno & Morrone, 2007).

Despite smaller peripheral biases for the nearest eccentricities in Experiment 2, the overall pattern of errors in the monocular viewing condition across the four axes tested matches that found in Experiment 1. Specifically, responses along all four axes showed an overall peripheral bias with monocular viewing. When the raw magnitude estimates were fit with power functions, results showed significant deviations from a value of 1 in the exponent and slope parameters of the right/temporal axis and the inferior axis, similar to those found in Experiment 1. In addition, estimates along the superior and left/nasal axes showed essentially a Euclidean mapping of space, with both exponent and slope parameters not significantly different from 1.

However, scaling was different for monocular and binocular viewing along the left axis, while biases were consistent across the two viewing conditions for the other three axes. For the left axis, the mean magnitude of errors with binocular viewing was similar in size to that found along the right axis in both viewing conditions. This finding supports the prediction that the nose provides an external boundary that changes the scaling of visual space. An external boundary could allow participants to make judgments about perceived location in an allocentric reference frame, where space is defined by the boundaries of the external borders. The absence of an external border would then force participants to make judgments relative to the intrinsic border defined by the edge of their visual field and to use an egocentric reference frame that is bounded by the edges of the visual field (i.e., a retinotopic reference frame).

However, there is a potential confound, as the region in which targets were presented along the left axis consisted solely of the nasal visual field for the right eye in the monocular viewing condition, while targets were presented in the nasal visual field of the right eye *and* the temporal visual field of the left eye in the binocular viewing condition. It is therefore possible that differences in spatial processing between the nasal and temporal visual fields (Curcio & Allen, 1990; Fahle & Schmid, 1988; Paradiso & Carney, 1988) could underlie some of the difference between monocular and binocular viewing in scaling along the left axis that we observed in Experiment 2. To address this possibility, we conducted Experiment 3, in which participants completed the same monocular and binocular tasks as in Experiment 2 in the presence of a constant external border consisting of an aperture edge placed in the Goldmann perimeter.

Experiment 3

Methods

Participants

Twelve undergraduates (9 females; mean age: 20.3 ± 3.2 years) who had not participated in the previous two experiments participated in this experiment for course credit. The same exclusion criteria from Experiment 1 were used.

Materials and procedure

Determination of visual field boundaries and stimulus presentation procedures were the same as in Experiment 2, with the addition of a ring-shaped aperture placed inside the Goldmann perimeter with an inner radius of 30° eccentricity. This aperture size was chosen to ensure that the inner edge of the aperture would be visible along all axes for all participants, given that upper visual field extents can be as small as 40° in some participants. Due to the curvature of the dome, the aperture was created by carefully layering 1.3 × 5.1 cm strips of black paper

around the dome. Strips were adhered such that the longer dimension was aligned in the radial direction. The first strips were adhered to the cardinal axes, with the longer dimension horizontally oriented for the left/right edges and vertically oriented for the upper/lower edges, as these were the axes along which the targets were presented. The rest of the aperture was then constructed by adhering additional strips of the same size that partially overlapped one another, one strip at a time, to create a continuous curved inner border without any visible boundaries between the strips. The use of multiple thin strips allowed for the creation of a ring-shaped aperture (15° thick) to be formed to the curvature of the dome.

For all participants and in both viewing conditions, the target was presented at seven eccentricities within the aperture, along each of the four cardinal axes. The eccentricities were 4°, 8°, 12°, 16°, 20°, 24°, and 28° of visual angle. Using the same method as Experiment 2, participants generated a verbal magnitude estimate of the target's location on every trial. The estimate ranged between 0 and 100, where 0 corresponded to the point of fixation and 100 corresponded to the inner edge of the aperture. Each of the 28 target locations was tested 5 times. Different random sequences of target location along all four axes were generated prior to testing for each participant and for each of the two viewing conditions. Trials with target locations along the four axes were intermixed within each block. Before each block, participants completed five practice trials at randomly chosen target locations. As in Experiment 2, monocular and binocular viewing conditions were tested in separate blocks, and block order was counterbalanced across participants.

Results

Localization errors

The mean measured visual extents of the participants' right eyes were: temporal axis = 88° ± 4°, nasal axis = 55° ± 7°, inferior axis = 69° ± 5°, superior axis = 50° ± 8°. The mean visual extents of the binocular visual fields were: right axis = 86° ± 4°, left axis = 86° ± 4°, inferior axis = 70° ± 6°, superior axis = 50° ± 11°. As participants judged target locations relative to the aperture edge, each target eccentricity was converted to percentage of distance between central fixation and the aperture edge. Errors in magnitude estimates were then calculated by subtracting the true target location (in units of percentage of aperture extent) from the corresponding magnitude estimates. Figure 8 shows the mean errors in percent of aperture extent as a function of target eccentricity and viewing condition for the vertical and horizontal meridians. Across all axes and both viewing conditions, participants showed a foveal bias. That is, participants tended to underestimate target eccentricity, and the magnitude of this underestimation was proportional to target eccentricity.

A 2 (Viewing Condition) × 4 (Axis) × 7 (Eccentricity) repeated measures ANOVA was conducted on mean localization errors, using Greenhouse–Geisser corrections when appropriate. There was a main effect of Viewing Condition ($F(1,11) = 5.08$, $p = 0.05$), with a larger foveal bias in the monocular compared to the binocular viewing condition. There were also main effects of Axis ($F(3,33) = 5.83$, $p = 0.003$) and Eccentricity ($F(1.47,16.16) = 3.92$, $p = 0.05$), with larger foveal biases at more peripheral eccentricities. The Axis × Eccentricity

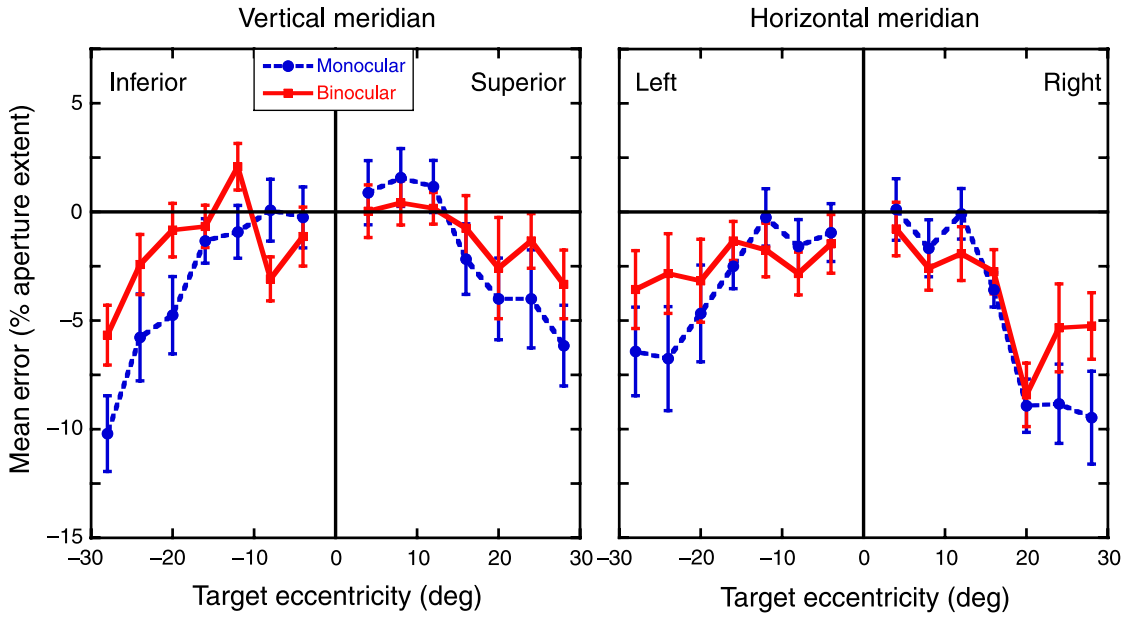

Figure 8. Experiment 3: Localization errors. Mean errors in percent of aperture extent for the vertical and horizontal meridians as a function of viewing condition and target eccentricity. Error bars represent *SEM*. The solid horizontal lines at zero represent expected performance if no distortion exists.

interaction was significant ($F(18,198) = 3.18$, $p < 0.001$), as was the Viewing Condition × Eccentricity interaction ($F(2.03,22.37) = 9.67$, $p = 0.001$). In contrast to Experiment 2, localization error differences across the two viewing conditions did not differ across the four axes tested, as indicated by the lack of either a significant Axis × Viewing Condition interaction ($F(3,33) = 1.20$, $p = 0.32$) or a significant three-way interaction ($F(18,198) = 1.33$, $p = 0.17$). A trend analysis of the Eccentricity factor showed no significant trends, though the linear trend approached significance (linear: $p = 0.06$, quadratic: $p = 0.13$, cubic: $p = 0.39$).

Magnitude scaling

The same hierarchical fitting procedure described in Experiment 1 was used here. The one-parameter model accounted for 92% of average variance (range: 55 to 98), and the two-parameter model accounted for 94% of average variance (range: 81 to 99). Overall, the two-parameter model provided a significantly better fit for only 40 of 96 (42%) cases. Moreover, for each axis and viewing condition individually, there was no clear bias toward one model providing a better fit across participants. As a result, subsequent analyses were conducted on the estimated slope parameters from the one-parameter (linear) model.[3]

Figure 9 shows the mean slope parameters for each of the four axes across the two viewing conditions. A 2 (Viewing Condition) × 4 (Axis) repeated measures ANOVA showed a main effect of Viewing Condition ($F(1,11) = 10.46$, $p = 0.008$), with monocular viewing having lower slopes for all axes. There was also a main effect of Axis ($F(3,33) = 6.01$, $p = 0.002$), but the Axis × Viewing Condition interaction was not significant ($F(3,33) = 1.24$, $p = 0.31$). Post-hoc comparisons, corrected for multiple comparisons, indicate that the main effect of Axis was driven by smaller slope estimates along the right compared to the superior axis (Sidak-adjusted value: $p = 0.05$). All other pairwise comparisons between the four axes failed to reach significance (all p values > 0.07). One-sample t tests were used to determine whether the slope parameters across the eight conditions differed significantly from a hypothetical mean of 1 using the Sidak–Bonferonni correction for multiple comparisons ($\alpha_{S-B} = 0.006$). For binocular viewing, mean slope estimates were significantly less than 1 only along the right axis (0.93, $p < 0.001$; other axes > 0.96, $p \geq 0.17$), while for monocular viewing, slopes were significantly less than 1 along all axes except for the superior axis (0.95, $p = 0.03$; other axes < 0.93, $p \leq 0.006$).

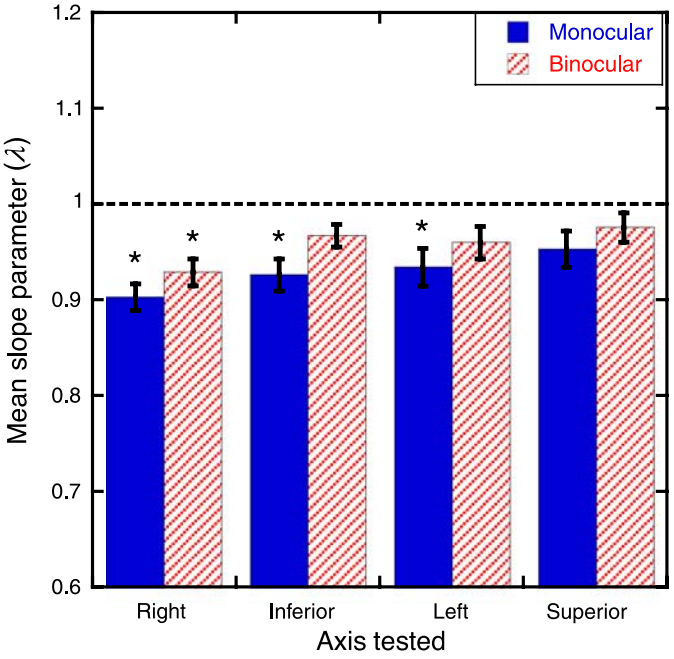

Figure 9. Experiment 3: Slope parameters. Mean estimated slope parameters as a function of viewing condition and axis tested, obtained from fitting individual magnitude estimates with the one-parameter function $J = \lambda D$. Error bars represent *SEM*. The dotted line at one represents expected performance if the mapping is undistorted and Euclidean. Asterisks indicate that the mean value is significantly different from 1, following correction for multiple comparisons.

Discussion

The results of this experiment indicate that in the presence of clear external visual field boundaries provided by an aperture edge, strong foveal biases and linear scaling of judgments as a function of eccentricity are present across all four cardinal axes. These findings provide further support that external borders aid in establishing a linear spatial metric that counters inherent peripheral biases in perceived location that occur when no boundaries are present. The slope estimates in the present experiment are similar to those found in a recent study in which participants judged target locations at the same eccentricities along the four cardinal axes relative to an aperture edge located at 30°, although the targets were presented on a computer monitor (see Figure 2; Fortenbaugh & Robertson, 2011). Unlike the results from Experiments 1 and 2 in which there was no aperture present, Experiment 3 revealed foveal biases that increase with eccentricity. The different pattern of errors across eccentricity due to the introduction of external boundaries and the switch from a peripheral to a foveal bias suggests that external boundaries such as the edge of an aperture or the edges of a computer monitor are a distinct class of boundaries from those created by the edges of the visual field.

In Experiment 2, patterns of localization bias and scaling were quite different for monocular and binocular viewing of targets along the left/nasal axis. In contrast, this distinction between monocular and binocular viewing was not evident in Experiment 3, where greater foveal

biases (for large eccentricities) and smaller slope estimates were observed in the monocular viewing condition than the binocular viewing condition across all four axes. These results suggest that inherent differences in spatial processing between nasal and temporal visual fields cannot explain the scaling differences between monocular (right eye) and binocular viewing along the left axis that were observed in Experiment 2.

The foveal biases observed in Experiment 3 also rule out the use of the Goldmann perimeter as the cause of the peripheral biases observed in Experiments 1 and 2. Previous studies of peripheral localization have used computer monitors (Adam, Ketelaars, Kingma, & Hoek, 1993; Bocianski et al., 2008; Bruno & Morrone, 2007; Fortenbaugh & Robertson, 2011; Kerzel, 2002; Sheth & Shimojo, 2004; Tsal & Bareket, 2005; van der Heijden et al., 1999), arrays of LEDs (Carrozzo, Stratta, McIntyre, & Lacquaniti, 2002; Enright, 1995; Lewald & Ehrenstein, 2000; Mateeff & Gourevich, 1983), and stereoscopic displays (Bock, 1993) for stimulus presentation. To our knowledge, only two studies have used a dome-shaped perimeter to conduct visual spatial localization experiments (Temme et al., 1985 and the present study). If the Goldmann perimeter had unique properties that led to peripheral biases (for example, the type of target light or the half-dome environment that eliminates any spatial cues from the surrounding testing room), this bias should have been evident in all three of our experiments. The fact that strong foveal biases were observed in Experiment 3 therefore supports the notion that it is the presence or absence of external visual field boundaries, not the Goldmann perimeter itself, which determines the type and magnitude of localization biases.

General discussion

We have found that borders that define visual space modulate biases in judging target location for stationary targets presented along the cardinal axes. Specifically, Experiment 1 showed that monocular target localization, as assessed with paper-and-pencil responses, exhibits a peripheral bias (replicating Temme et al., 1985). Non-linear regression analyses demonstrated that the spatial scaling along the temporal and inferior axes was different than scaling along the nasal and superior axes. The existence of external facial boundaries in the visual field accounts for these differences: for monocular viewing, the nasal axis (nose) and superior axis (brow) have visibly prominent boundaries, and these are the axes exhibiting linear scaling of target location. In contrast, scaling was non-linear along the temporal and inferior axes where intrinsic visual field boundaries were present. Thus, these results provide evidence that external visual boundaries change not only the reference frame in which localization occurs (as suggested by Sheth & Shimojo, 2004) but also the spatial metric within the reference frame.

In Experiment 2, we tested whether the same localization biases observed with paper-and-pencil responses in Experiment 1 were evident when participants responded with a verbal magnitude estimate. For monocular viewing, the results replicated the findings of Experiment 1: peripheral biases for all four axes, linear scaling for nasal and superior axes, and non-linear scaling for temporal and inferior axes. Thus, the patterns of localization bias and scaling are independent of response mode, at least with respect to the two response modes utilized in this study. However, it is possible that other response modes would produce a different pattern of localization errors. Importantly, our finding of peripheral bias when using a verbal magnitude estimate and the similarity in the pattern of errors across Experiments 1 and 2 demonstrate that peripheral biases are not limited to open-loop pointing responses, as has previously been suggested (Uddin, 2006).

Experiment 2 also contained a binocular viewing condition to eliminate the nose as an external visual field boundary, and this produced a significant increase in the magnitude of peripheral bias along the left axis, compared to monocular viewing, as well as a change in scaling from a linear to a non-linear metric. Experiment 3 provides further support for the role of external visual boundaries in the scaling of visual space. Here, the presence of a strong external border (an aperture edge) caused a consistent foveal bias and linear scaling of visual space across all four axes in both monocular and binocular viewing conditions.

Theories of location perception for stationary targets have predominately focused on the effects of eye movements and attention on the accuracy of responses (Adam et al., 2008, 1993; Tsal & Shalev, 1996; Uddin, 2006). Adam et al. (1993; Adam, Paas, Ekering, & Loon, 1995) proposed a two-process model for localization of stationary targets, in which the movement of attention toward targets provides coarse location information that is further refined with eye movements that are made toward the target. One limitation of the two-process model is that it fails to predict whether a foveal or peripheral bias should occur in a given task, as the model focuses on absolute accuracy rather than bias. One proposal to account for biases is that the dissociation between the point of fixation and the locus of covert attention determines the direction of biases in spatial localization tasks, at least using perceptual reports (Uddin, 2006; Uddin et al., 2005a; Uddin, Kawabe, & Nakamizo, 2005b). According to this model, when fixation is maintained centrally and a peripheral target is presented, attention is focused at the point of fixation, resulting in a foveal bias in perceived location. However, to the extent that attention is also drawn to objects at more eccentric locations than the target, perceived target location will be determined by the degree of allocation of attention to the relative locations of the fixation point and distracter object, leading to a possible peripheral bias. While attention has been shown

to modulate localization errors of stationary targets (Adam et al., 2008; Bocianski, Müsseler, & Erlhagen, 2010; Fortenbaugh & Robertson, 2011; Tsal & Bareket, 2005; Yamada, Kawabe, & Miura, 2008), attentional weighting cannot explain the influence of visual field boundaries on either the scaling or type of biases that we have observed in the present study, as the degree to which borders were attended presumably did not vary across the axes tested. In addition, the attentional demands and task were identical in Experiments 2 and 3, but the direction of localization bias was different in these two experiments.

When attention is drawn to landmarks at a greater eccentricity than the target, estimates of target location can be peripherally displaced toward the landmark location (Uddin et al., 2005a; Yamada et al., 2008). In the present study, participants were required to allocate attention to both the fixation point and either the edges of the visual field (Experiments 1 and 2) or the inner edge of the aperture (Experiment 3) in order to determine the relative position of targets along the length of an axis. This is due to the nature of the tasks, both of which required participants to first assess the length of the tested axis and then to generate a magnitude estimate based on the perceived distance of the targets from fixation relative to the perceived length of the axis. However, it seems unlikely that the edges of the visual field or the aperture influenced responses in the same way as the landmark/distracter objects used in previous studies (Kerzel, 2002; Sheth & Shimojo, 2004; Uddin et al., 2005a). First, the aperture in Experiment 3 provided the most salient edge, while the least salient edge was provided by the temporal and inferior visual fields in Experiments 1 and 2. However, the former condition produced the largest foveal bias, and the latter conditions resulted in the largest peripheral biases. Second, the effect of landmarks diminishes with distance from the target location (Uddin et al., 2005a). However, the largest foveal biases we observed were for the most peripheral target locations closest to the edge of the aperture (Experiment 3), while peripheral biases diminished or switched to foveal biases as target location approached the edge of the visual field in Experiments 1 and 2.

An alternative account of our findings is that different reference frames can be used to assess the location of a single stationary target depending on task demands and that the type of reference frame used can lead to variations in perceived location (Sheth & Shimojo, 2004; Uddin, 2006). The idea that multiple, hierarchical reference frames can coexist and have differing consequences for spatial localization is well established (Bridgeman, 1999; Bridgeman, Peery, & Anand, 1997; Lemay & Stelmach, 2005; Paillard, 1991; Robertson, 2004). In a peripheral localization task, observers rely more on extrinsic than intrinsic reference frames to determine target location, even when this information is unreliable (Sheth & Shimojo, 2004). In our Experiments 1 and 2, the axes varied in the type of visual field border. One account of our results is that an egocentric reference frame is used to make location judgments relative to intrinsic visual boundaries (producing peripheral localization biases), while external visual boundaries, provided either by visible facial features or a physical aperture, results in the use of an allocentric reference frame.

Our measurements of spatial scaling also support the association of intrinsic visual boundaries with an egocentric reference frame and of external boundaries with an allocentric reference frame. In this framework, target location is initially encoded within a retinotopic (egocentric) reference frame. Peripheral biases and non-linear scaling are consistent with known distortions in the representation of the visual field in retinotopically organized visual areas that contain an overrepresentation of the central visual field (Horton & Hoyt, 1991). The introduction of external boundaries may allow for a linearization of space across eccentricity and ultimately a switch from a peripheral to a foveal bias, depending on the degree to which boundaries enclose a region that is separate from the observer (i.e., the partial border provided by the brow and nose versus the border provided by the aperture that fully enclosed a region of visual space in all directions).

In conclusion, the results of the present study demonstrate that the type of visual field boundary present can significantly alter the perceived locations of stationary targets in the peripheral visual field. Further exploration of the effects of visual boundaries on spatial localization will help elucidate not only the types of reference frames used in spatial localization but also the spatial metrics within these reference frames.

Acknowledgments

This research was supported by the Veterans Administration, National Institutes of Health Grant R01-EY016975 (L.C.R.), the Chancellor's Faculty Partnership Fund at the University of California, Berkeley (L.C.R. and M.A.S.), an NSF-GRF (F.C.F.), NIH Training Grant T35-EY007139 (S.S.), and NEI Core Grant EY003176. Lynn C. Robertson has a Senior Research Career Scientist Award from the Veterans Administration and is affiliated with the VA Clinical Sciences Research Service, Department of Veterans Affairs Medical Center, Martinez, CA. The authors thank Alyssa Beck and Betty Wang for help with data collection.

Commercial relationships: none.
Corresponding author: Lynn C. Robertson.
Email: lynnrob@berkeley.edu.
Address: Department of Psychology, 4143 Tolman Hall #5050, University of California, Berkeley, CA 94720, USA.

Footnotes

[1]A Goldmann perimeter (Figure 1) is a self-illuminated half-dome with a uniform white background and is used for kinetic perimetry.

[2]While differences in perception between the left and right hemispheres have been reported for a variety of dimensions (Charles, Sahraie, & McGeorge, 2007; Toba, Cavanagh, & Bartolomeo, 2011), hemispheric specialization cannot explain all of our findings. In particular, hemispheric specialization predicts differences in localization solely between the left and right sides of a display and not between the upper and lower vertical meridians. In contrast, in the present study, we found one type of scaling for the temporal (right) and inferior axes and a different type of scaling for the nasal (left) and superior axes.

[3]Analyses were also conducted on the model fits for the two-parameter model. Results showed that the estimated exponent parameters for all four axes across both viewing conditions failed to differ from a value of 1, confirming that selection of the one-parameter linear model is appropriate for this experiment.

References

Adam, J. J., Davelaar, E. J., van der Gouw, A., & Willems, P. (2008). Evidence for attentional processing in spatial localization. *Psychological Research, 72,* 433–442. [PubMed]

Adam, J. J., Ketelaars, M., Kingma, H., & Hoek, T. (1993). On the time course and accuracy of spatial localization: Basic data and a two-process model. *Acta Psychologica, 84,* 135–159. [PubMed]

Adam, J. J., Paas, F. G. W. C., Ekering, J., & Loon, E. M. (1995). Spatial localization: Tests of a two-process model. *Experimental Brain Research, 102,* 531–539. [PubMed]

Bocianski, D., Müsseler, J., & Erlhagen, W. (2008). Relative mislocalization of successively presented stimuli. *Vision Research, 48,* 2204–2212. [PubMed]

Bocianski, D., Müsseler, J., & Erlhagen, W. (2010). Effects of attention on a relative mislocalization with successively presented stimuli. *Vision Research, 50,* 1793–1802. [PubMed]

Bock, O. (1993). Localization of objects in the peripheral visual field. *Behavioural Brain Research, 56,* 77–84. [PubMed]

Bridgeman, B. (1999). Separate representations of visual space for perception and visually guided behavior. In G. Aschersleben, T. Bachmann, & J. Musseler (Eds.), *Advances in psychology* (vol. 129, pp. 3–13). Amsterdam, Netherlands: North-Holland/Elsevier Science Publishers.

Bridgeman, B., Peery, S., & Anand, S. (1997). Interaction of cognitive and sensorimotor maps of visual space. *Perception & Psychophysics, 59,* 456–469. [PubMed]

Bruno, A., & Morrone, M. C. (2007). Influence of saccadic adaptation on spatial localization: Comparison of verbal and pointing errors. *Journal of Vision, 7*(5):16, 1–13, http://www.journalofvision.org/content/7/5/16, doi:10.1167/7.5.16. [PubMed] [Article]

Carrozzo, M., Stratta, F., McIntyre, J., & Lacquaniti, F. (2002). Cognitive allocentric representations of visual space shape pointing errors. *Experimental Brain Research, 147,* 426–436. [PubMed]

Charles, J., Sahraie, A., & McGeorge, P. (2007). Hemispatial asymmetries in judgment of stimulus size. *Perception & Psychophysics, 69,* 687–698. [PubMed]

Curcio, C. A., & Allen, K. A. (1990). Topography of ganglion cells in human retina. *The Journal of Comparative Neurology, 300,* 5–25. [PubMed]

Cutting, J. E., & Vishton, P. M. (1995). Perceiving layout and knowing distances: The integration, relative potency, and contextual use of different information about depth. In W. E. S. Rogers (Ed.), *Handbook of perception and cognition* (vol. 5, pp. 69–117). San Diego, CA: Academic Press.

Enright, J. T. (1995). The non-visual impact of eye orientation on eye–hand coordination. *Vision Research, 35,* 1611–1618. [PubMed]

Fahle, M., & Schmid, M. (1988). Naso-temporal asymmetry of visual perception and of the visual cortex. *Vision Research, 28,* 293–300. [PubMed]

Fortenbaugh, F. C., Hicks, J. C., Hao, L., & Turano, K. A. (2007). Losing sight of the bigger picture: Peripheral field loss compresses representations of space. *Vision Research, 47,* 2506–2520. [PubMed] [Article]

Fortenbaugh, F. C., & Robertson, L. C. (2011). When here becomes there: Attentional distribution modulates foveal bias in peripheral localization. *Attention, Perception, & Psychophysics, 73,* 809–828. [PubMed] [Article]

Gibson, J. J. (1950). *The perception of the visual world.* Westport, CT: Greenwood Press.

He, Z. J., Wu, B., Ooi, T. L., Yarbrough, G., & Wu, J. (2004). Judging egocentric distance on the ground: Occlusion and surface integration. *Perception, 33,* 789–806. [PubMed]

Horton, J. C., & Hoyt, W. F. (1991). The representation of the visual field in human striate cortex: A revision of

the classic Holmes map. *Archives of Ophthalmology, 109,* 816–824. [PubMed]

Hubbard, T. L. (2005). Representational momentum and related displacements in spatial memory: A review of the findings. *Psychonomic Bulletin & Review, 12,* 822–851. [PubMed]

Hubbard, T. L., & Ruppel, S. E. (2000). Spatial memory averaging, the landmark attraction effect, and representational gravity. *Psychological Research, 64,* 41–55. [PubMed]

Kerzel, D. (2002). Memory for the position of stationary objects: Disentangling foveal bias and memory averaging. *Vision Research, 42,* 159–167. [PubMed]

Kerzel, D., & Gegenfurtner, K. R. (2004). Spatial distortions and processing latencies in the onset repulsion and Fröhlich effects. *Vision Research, 44,* 577–590. [PubMed]

Lemay, M., & Stelmach, G. E. (2005). Multiple frames of reference for pointing to a remembered target. *Experimental Brain Research, 164,* 301–310. [PubMed]

Lewald, J., & Ehrenstein, W. H. (2000). Visual and proprioceptive shifts in perceived egocentric direction induced by eye-position. *Vision Research, 40,* 539–547. [PubMed]

Low, F. N. (1951). Peripheral visual acuity. *Archives of Ophthalmology, 45,* 80–99. [PubMed]

Luneburg, R. K. (1950). Metric of binocular visual space. *Journal of the Optical Society of America, 40,* 627–642.

Mateeff, S., & Gourevich, A. (1983). Peripheral vision and perceived visual direction. *Biological Cybernetics, 49,* 111–118. [PubMed]

Motulsky, H., & Christopoulos, A. (2004). *Fitting models to biological data using linear and nonlinear regression: A practical guide to curve fitting*. New York: Oxford University Press.

Müsseler, J., & Van der Heijden, A. C. H. (2004). Two spatial maps for perceived visual space: Evidence from relative mislocalization. *Visual Cognition, 11,* 235–254.

Müsseler, J., van der Heijden, A. C. H., Mahmud, S. H., Deubel, H., & Ertsey, S. (1999). Relative mislocalization of briefly presented stimuli in the retinal periphery. *Perception & Psychophysics, 61,* 1646–1661. [PubMed]

Ooi, T. L., Wu, B., & He, Z. J. (2001). Distance determined by the angular declination below the horizon. *Nature, 414,* 197–200. [PubMed]

Ooi, T. L., Wu, B., & He, Z. J. (2006). Perceptual space in the dark affected by the intrinsic bias of the visual system. *Perception, 35,* 605–624. [PubMed]

Paillard, J. (1991). Motor and representation framing of space. In J. Paillard (Ed.), *Brain and science* (pp. 163–182). Oxford, UK: Oxford University Press.

Palmer, S. (1999). *Vision science: Photons to phenomenology*. Cambridge, MA: The MIT Press.

Paradiso, M. A., & Carney, T. (1988). Orientation discrimination as a function of stimulus eccentricity and size: Nasal/temporal retinal asymmetry. *Vision Research, 28,* 867–874. [PubMed]

Philbeck, J. W., Loomis, J. M., & Beall, A. C. (1997). Visually perceived location is an invariant in the control of action. *Perception & Psychophysics, 59,* 601–612. [PubMed]

Randall, H. G., Brown, D. J., & Sloan, L. L. (1966). Peripheral visual acuity. *Archives of Ophthalmology, 75,* 500–504. [PubMed]

Robertson, L. (2004). *Space, objects, minds and brains*. New York, NY: Psychology Press.

Rose, D., & Halpern, D. L. (1992). Stimulus mislocalization depends on spatial frequency. *Perception, 21,* 289–296. [PubMed]

Sheth, B. R., & Shimojo, S. (2004). Extrinsic cues suppress the encoding of intrinsic cues. *Journal of Cognitive Neuroscience, 16,* 339–350. [PubMed]

Sinai, M. J., Ooi, T. L., & He, Z. J. (1998). Terrain influences the accurate judgement of distance. *Nature, 395,* 497–500. [PubMed]

Steel, S. E., Mackie, S. W., & Walsh, G. (1996). Visual field defects due to spectacle frames: Their prediction and relationship to UK driving standards. *Ophthalmic and Physiological Optics, 16,* 95–100. [PubMed]

Temme, L. A., Maino, J. H., & Noell, W. K. (1985). Eccentricity perception in the periphery of normal observers and those with retinitis pigmentosa. *American Journal of Optometry and Physiological Optics, 62,* 736–743. [PubMed]

Thornton, I. M. (2002). The onset repulsion effect. *Spatial Vision, 15,* 219–243. [PubMed]

To, M. P. S., Regan, B. C., Wood, D., & Mollon, J. D. (2011). Vision out of the corner of the eye. *Vision Research, 51,* 203–214. [PubMed]

Toba, M.-N., Cavanagh, P., & Bartolomeo, P. (2011). Attention biases the perceived midpoint of horizontal lines. *Neuropsychologia, 49,* 238–246. [PubMed]

Tsal, Y., & Bareket, T. (2005). Localization judgments under various levels of attention. *Psychonomic Bulletin & Review, 12,* 559–566. [PubMed]

Tsal, Y., & Shalev, L. (1996). Inattention magnifies perceived length: The attentional receptive field hypothesis. *Journal of Experimental Psychology: Human Perception and Performance, 22,* 233–243. [PubMed]

Turano, K. A. (1991). Bisection judgements in patients with retinitis pigmentosa. *Clinical Vision Sciences, 6,* 119–130.

Uddin, M. K. (2006). Visual spatial localization and the two-process model. *Kyushu University Psychological Research, 7,* 65–75.

Uddin, M. K., Kawabe, T., & Nakamizo, S. (2005a). Attention shift not memory averaging reduces foveal bias. *Vision Research, 45,* 3301–3306. [PubMed]

Uddin, M. K., Kawabe, T., & Nakamizo, S. (2005b). Differential roles of distracters in reflexive and memory-based localization. *Spatial Vision, 18,* 579–592. [PubMed]

van der Heijden, A., van der Geest, J., de Leeuw, F., Krikke, K., & Müsseler, J. (1999). Sources of position-perception error for small isolated targets. *Psychological Research, 62,* 20–35. [PubMed]

Wittich, W., Faubert, J., Watanabe, D. H., Kapusta, M. A., & Overbury, O. (2011). Spatial judgments in patients with retinitis pigmentosa. *Vision Research, 51,* 165–173. [PubMed]

Yamada, Y., Kawabe, T., & Miura, K. (2008). Mislocalization of a target toward subjective contours: Attentional modulation of location signals. *Psychological Research, 72,* 273–280. [PubMed]